Supporting Information

Peroxynitrite-Biosignal-Responsive Polymer Micelles as Intracellular Hypersensitive Nanoprobes

Xi Liu,[a,b] Jiannan Zhu,[a] Kunbing Ouyang,*[b] and Qiang Yan*[a]

[1]*State Key Laboratory of Molecular Engineering of Polymers, Fudan University, Shanghai, China 200433.*
[2]*Key Laboratory of Environmentally Friendly Chemistry and Applications of Ministry of Education College of Chemistry, Xiangtan University, Xiangtan, China 411105*

Corresponding author: yanq@fudan.edu.cn

Table of Contents

1. General.

3-(4-Methoxyphenyl) propanoic acid (Sigma, 99%), trifluoromethyl trimethylsilane ($TMSCF_3$, J&K, 99.5%), Tetrabutylammonium fluoride (TBAF, Sigma, 99%), boron tribromide (BBr_3, Sigma, 98%), methacrylic acid (MAA, J&K, 98%), 4-dimethylamino pyridine (DMAP, Acros, 98%), 1-ethyl-3-(3-dimethylaminopropyl)carbodiimide (EDC, Acros, 99%), 2-bromoisobutylryl bromide (BiBB, Sigma, 99%), triethylamine (TEA, Sigma, 98%), 2,2'-bipyridine (bpy, Adamas, 99.5%), copper (I) bromide (CuBr, Sigma, 99.9%), 5-carboxytetramethyl rhodamine succinimidyl ester (TMR, Sigma, 99%), 3-morpholinosydnonimine (SIN-1, Sigma, 98%) and cesium fluoride (CsF, Adamas, 98%) were used as received. Methoxy poly(ethylene oxide)-based macro-initiator (PEO-Br, $M_{n,GPC}$ = 2.3 kDa, M_w/M_n = 1.02) was prepared according to the literature elsewhere.[1]

Nuclear Magnetic Resonance (NMR). ^{1}H NMR, ^{13}C NMR and ^{19}F NMR spectra for the monomer and final block copolymer samples were recorded by AVANCE III HD-400 (400 MHz) spectrometer with $CDCl_3$ or d_8-THF/D_2O as the solvent.

Gel Permeation Chromatography (GPC). The molecular weight and polydispersity of all polymer samples were measured on a system of multiangle laser light scattering. The system is equipped with a Waters degasser, a Waters 515 HPLC pump, a Wyatt Optilab DSP differential refractometer and a Wyatt miniDAWN detector. HPLC-grade dimethylformamide (DMF) with 0.1 M LiBr was used as eluent at a flow rate of 1.0 mL min^{-1} at 30 ^{o}C and poly(ethylene oxide) as a standard reference.

Transmission Electron Microscopy (TEM). TEM images were measured on a FEI Tecnai G2-F20 S-TWIN instrument at a voltage of 120 kV. The specimens were prepared by drop-casting polymer aggregates solution (10 μL) onto carbon-coated grid and freeze-drying before observation.

UV-Vis Spectroscopy (UV-Vis). UV-Vis absorption spectra of the MATFK monomer (10 μM) with equal molar $ONOO^-$ (10 μM in PBS buffer, pH=7.4) were recorded by using an Agilent Cary-60 UV-Vis spectroscopy at given time intervals. The turbidity of the polymer assemblies (1.8×10^{-4} g L^{-1}) upon various $ONOO^-$ stimuli conditions (1.0, 0.7 and 0.4 equiv.) were analyzed at 550 nm wavelength.

Fluorescent Spectroscopy (FS). The fluorescent changes of PEO-*b*-P(MATFK-*co*-TMR) polymer nanoparticles (1.8×10^{-4} g L^{-1}) upon treatment with various concentrations of $ONOO^-$ were conducted by a SHIMADZU RF-5301PC fluorescent spectroscopy.

Dynamic Light Scattering (DLS). The hydrodynamic diameter (D_h) changes of the different polymer assemblies in aqueous solution were conducted on a Brookhaven (BI-200SM) system equipped with a sensitive avalanche photodiode detector (BI-APD), a digital correlator (TurboCorr). The scattering angel is fixed on 90^o for all the aggregates. Before the DLS measurements, the polymer solution were filtered.

Confocal Laser Scanning Microscope (CLSM). For confocal imaging in live cells, endothelial cells were cultured on glass-bottom 6-well plates overnight, then incubated with PEO-*b*-P(MATFK-*co*-TMR) polymer nanoparticles (1.8×10^{-4} g L^{-1}) at 37 ^{o}C for 30 min. Then the changes of the polymer nanoparticulate fluorescence in live cells with different concentrations of 3-morpholinosydnonimine (SIN-1, a stable $ONOO^-$ donor reagent at 0 nM, 10 nM, 50 nM and 100 nM, respectively) stimulus were captured by confocal microscope (Nikon C2$^+$) for 30 min.

Mass Spectroscopy (HR ESI-MS). The molecular weight of the functional monomer was measured

on a high-resolution electrospray ionization mass spectrometry (Bruker McriOTOF11).

2. Synthesis and Preparation.

2.1 Synthesis of $ONOO^-$ Specific-Responsive Functional Monomer (MATFK)

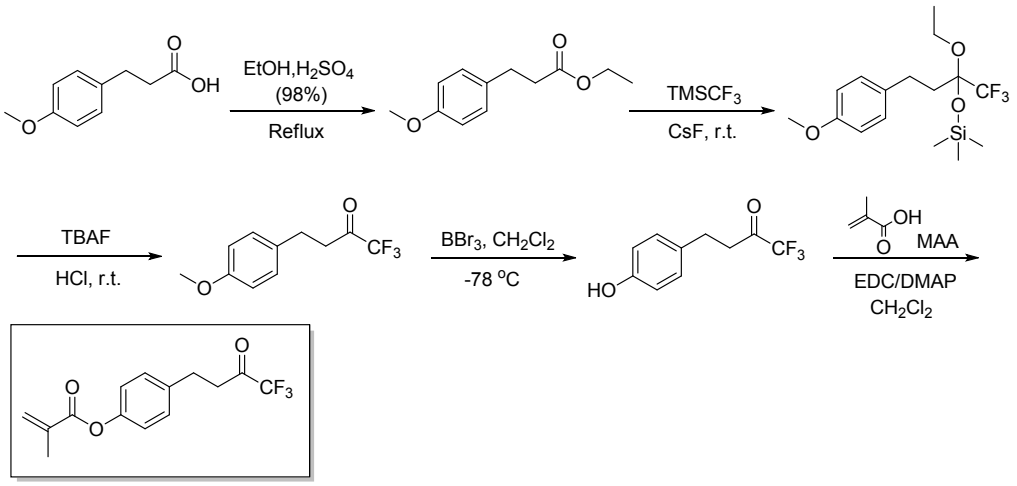

Scheme S1. Synthetic route of $ONOO^-$ responsive functional monomer, 4-(trifluoro-3-oxobutyl) phenyl methacrylate (**MATFK**)

Synthesis of ethyl 3-(4-methoxyphenyl) propanoate.
To a solution of 3-(4-methoxyphenyl) propanoic acid (5.10 g, 28.3 mmol) in ethanol (40 mL) was added H_2SO_4 (1.4 mL, 98%). The mixture was refluxed for 12 h. Then ethanol was removed under reduced pressure, and the residue was added ethyl acetate (50 mL). The resulting solution was treated with H_2O (50 mL), saturated sodium bicarbonate and saturated sodium chloride, respectively. The organic phase was dried with anhydrous Na_2SO_4, and then concentrated under reduced pressure, which obtained 3-(4-methoxyphenyl) propanoate (yield: 5.62 g, 95%; *Figure S1–S2*).

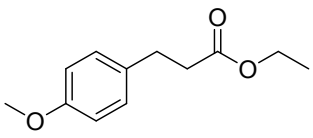

^{1}H NMR (δ, ppm, $CDCl_3$): 7.11-7.13 (d, J = 8.8 Hz, 2H, benzene), 6.82-6.84 (d, J = 8.7 Hz, 2H, benzene), 4.09-4.15 (q, J = 7.1 Hz, 2H, $CH_3C\boldsymbol{H}_2O$-), 3.77 (s, 3H, $C\boldsymbol{H}_3O$-), 2.87-2.91 (t, J = 7.5 Hz, 2H, -$C\boldsymbol{H}_2CH_2COO$-), 2.56-2.60 (t, J = 7.5 Hz, 2H, -$CH_2C\boldsymbol{H}_2COO$-), 1.22-1.25 (t, J = 7.1 Hz, 3H, $C\boldsymbol{H}_3CH_2O$-).

^{13}C NMR (δ, ppm, $CDCl_3$): 173.0, 158.0, 132.7, 129.3, 113.9, 60.4, 55.2, 36.3, 30.1, 14.2.

Synthesis of (2-ethoxytrifluoro-(4-methoxyphenyl)butan-2-yl) trimethylsilane.
To a solution of 3-(4-methoxyphenyl) propanoate (5.62 g, 27.0 mmol) and $TMSCF_3$ (6.0 mL, 40.5 mmol) was added CsF (41.0 mg, 0.27 mmol). The mixture was stirred at room temperature for 12 h and then hexane (30 mL) was added to the resulting solution, the mixture was washed with water and saturated sodium chloride respectively. The organic phase was dried with Na_2SO_4, and then was concentrated under reduced pressure. The residue was purified by silica gel column chromatography (hexane) to obtain (2-ethoxytrifluoro-(4-methoxyphenyl)butan-2-yl) trimethylsilane. (yield: 8.33 g, 88%; *Figure S3–S4*).

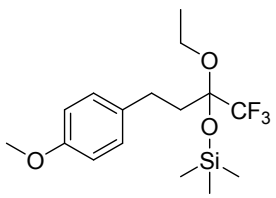

^{1}H NMR (δ, ppm, $CDCl_3$): 7.13-7.15 (d, J = 8.7 Hz, 2H, benzene), 6.85-6.87 (d, J = 8.6 Hz, 2H, benzene), 3.81 (s, 3H, $C\boldsymbol{H}_3OCCHCH$-), 3.66-3.74 (m, 2H,

$CH_3C\boldsymbol{H}_2OC$-), 2.67-2.74 (m, 2H, -$C\boldsymbol{H}_2CH_2CO$-), 2.00-2.15 (m, 2H, -$CH_2C\boldsymbol{H}_2CO$-), 1.24-1.28 (t, J = 7.0 Hz, 3H, $C\boldsymbol{H}_3CH_2OC$-), 0.24 (s, 9H, $C\boldsymbol{H}_3Si$-).

^{13}C NMR (δ, ppm, $CDCl_3$): 158.1, 133.6, 129.3, 125.1, 114.1, 98.0, 59.3, 55.4, 36.2, 28.0, 15.6, 1.7.

^{19}F NMR (δ, ppm, $CDCl_3$): -79.99.

Synthesis of trifluoro-4-(4-methoxyphenyl) butan-2-one.

The above products (8.00 g, 22.9 mmol) was added TBAF (1 M in THF, 30 mL) dropwise. The mixture was stirred at room temperature for 8 h and then was treated with hydrochloric acid (4.0 M, 10 mL) for 5 h. Ethyl acetate (30 mL) was added to the resulting solution, which was washed with water, saturated sodium bicarbonate and saturated sodium chloride respectively. The organic phase was dried with anhydrous Na_2SO_4, and then was concentrated under reduced pressure. The residue was purified by silica gel column chromatography (hexane/ethyl acetate 20:1) to obtain trifluoro-4-(4-methoxyphenyl)butan-2-one (yield: 5.22 g, 98%; *Figure S5–S6*).

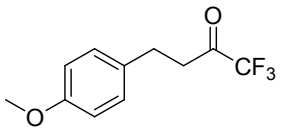

^1H NMR (δ, ppm, $CDCl_3$): 7.10-7.13 (d, J = 8.8 Hz, 2H, benzene), 6.83-6.85 (d, J = 8.7 Hz, 2H, benzene), 3.79 (s, 3H, $C\boldsymbol{H}_3OCCHCH$-), 3.02-3.04 (m, 2H, -$C\boldsymbol{H}_2CH_2COCF_3$), 2.91-2.94 (m, 2H, -$CH_2C\boldsymbol{H}_2COCF_3$).

^{13}C NMR (δ, ppm, $CDCl_3$): 190.6, 158.4, 131.3, 129.3, 117.0, 114.1, 55.2, 38.4, 27.5.

^{19}F NMR (δ, ppm, $CDCl_3$): -79.33.

Synthesis of trifluoro-4-(4-hydroxyphenyl) butan-2-one

To a solution of trifluoro-4-(4-methoxyphenyl) butan-2-one (5.22 g, 22.5 mmol) in CH_2Cl_2 (20 mL) was added BBr_3 (12 mL, 31.2 mmol) dropwise slowly at -78 ^oC under argon. The mixture was then warmed to room temperature and stirred overnight. After ice water (20 mL) was added slowly to the resulting solution, ethyl acetate (50 mL) was added subsequently. The mixture was treated with water, saturated sodium bicarbonate and saturated sodium chloride respectively. The organic phase was dried with Na_2SO_4 and the solvent was removed in vacuum to give a brown oily liquid which was purified by silica gel column chromatography (hexane/ethyl acetate 4:1) to yield trifluoro-4-(4-hydroxyphenyl) butan-2-one (yield: 4.23 g, 86%; *Figure S7–S8*).

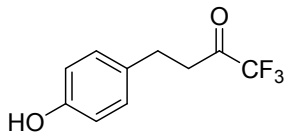

^1H NMR (δ, ppm, $CDCl_3$): 7.06-7.08 (d, J = 8.6 Hz, 2H, benzene), 6.76-6.78 (d, J = 8.6 Hz, 2H, benzene), 4.64 (br, 1H, $\boldsymbol{H}OCCHCH$-), 2.99-3.03 (m, 3H, -$C\boldsymbol{H}_2CH_2COCF_3$), 2.91-2.94 (m, 2H, -$CH_2C\boldsymbol{H}_2COCF_3$).

^{13}C NMR (δ, ppm, $CDCl_3$): 191.5, 154.0, 131.6, 121.8, 115.7, 38.3, 27.4.

^{19}F NMR (δ, ppm, $CDCl_3$): -79.26.

Synthesis of 4-(trifluoro-3-oxobutyl) phenyl methacrylate (MATFK)

Trifluoro-4-(4-hydroxyphenyl) butan-2-one (1.0 g, 4.59 mmol) in CH_2Cl_2 (30 mL) was added EDC (1.0 g, 5.25 mmol), DMAP (145 mg, 1.2 mmol) and methacrylic acid (410 mg, 4.8 mmol) at room temperature under Ar. After the solution was stirred overnight the reaction mixture was quenched with saturated sodium bicarbonate and then extracted with DCM three times. The resulting organic phase was washed with saturated sodium chloride and dried with Na_2SO_4, the solvent was concentrated under reduced pressure. The residue was purified by silica gel column chromatography

(hexane/ethyl acetate 4:1) to obtain 4-(trifluoro-3-oxobutyl) phenyl methacrylate (yield: 0.62 g, 47%; *Figure S9–S10*).

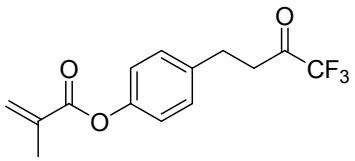

^{1}H NMR (δ, ppm, $CDCl_3$): 7.21-7.23 (d, J = 8.7 Hz, 2H, benzene), 7.05-7.07 (d, J = 8.6 Hz, 2H, benzene), 6.34 (m, 1H, C***H*****$_2$**=C(CH_3)), 5.76 (m, 1H, C***H*****$_2$**=CH(CH_3)), 3.04-3.07 (m, 2H, -C***H*****$_2$**CH_2COCF_3), 2.97-3.01 (m, 2H, -CH_2C***H*****$_2$**$COCF_3$), 2.06-2.07 (m, 3H, C***H*****$_3$**-).

^{13}C NMR (δ, ppm, $CDCl_3$): 190.7, 165.9, 149.6, 136.8, 135.8, 129.3, 127.3, 121.8, 117.0, 37.9, 27.6, 18.2.

^{19}F NMR (δ, ppm, $CDCl_3$): -79.30.

HR ESI-MS: calcd for $[C_{14}H_{14}O_3F_3 + H]^+$ 287.0895; found 287.0899.

3.2 Synthesis of Poly(ethylene oxide)-*block*-PMATFK Diblock Copolymer (PEO-*b*-PMATFK) and Fluorescent Copolymer PEO-*b*-P(MATFK-*co*-TMR) via ATRP method

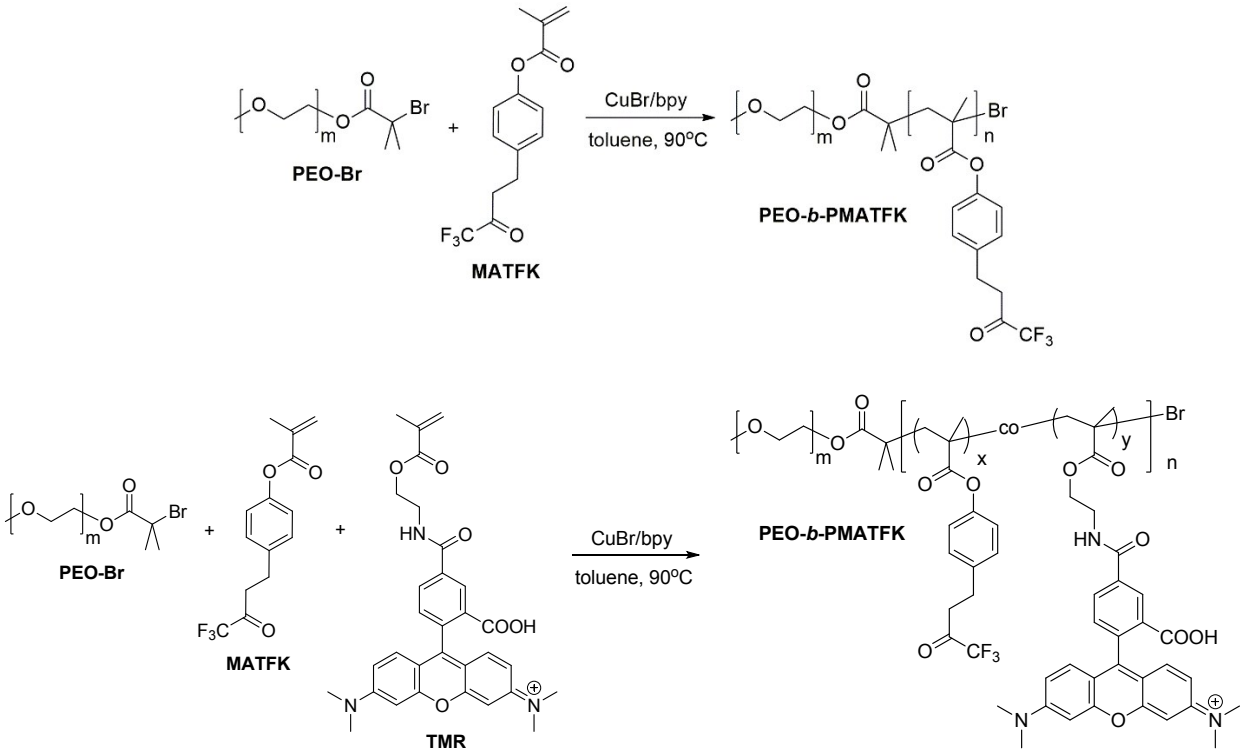

Scheme S2. Synthetic route of peroxynitrite specific-responsive amphiphilic block copolymer **PEO-*b*-PMATFK** (top) **and PEO-*b*-P(MATFK-*co*-TMR)** (bottom) via ATRP method.

The PEO-Br macro-initiator in toluene solution was added CuBr, 2,2'-bipyridine (bpy) ligand and MATFK monomer with the molar ratio of [CuBr]/[bpy]/[MATFK] = 1/1/100. Followed by three freeze-vacuum-thaw cycles, the reactive tube was heated at 90 °C with magnetic stirring for a given time. After the setting reaction time, the flask was immersed to liquid nitrogen to stop the radical polymerization. Then removing toluene in vacuum, the residue was dissolved in THF and dialyzed until the monomer was isolated completely (monitored by UV-Vis spectroscopy). The resulted solution was evaporated in vacuum and the target PEO-*b*-PMATFK copolymers were obtained. The results were listed in the following *Figure S11–S12 and Table S1*.

In a similar way, the fluorescent block copolymer PEO-*b*-P(MATFK-*co*-TMR) was prepared by the molar ratio of [CuBr]/[bpy]/[MATFK]/[TMR] = 1/1/90/10. The TMR fluorescent monomer was

synthesized according to the literature elsewhere.[2] The synthetic process and purification is in a same manner.

^{1}H NMR (δ, ppm, $CDCl_3$): 7.13–7.26 (s, in benzene), 6.96–7.00 (s, in benzene), 3.64 (s, -C***H***$_2$C***H***$_2$O- in PEO block), 3.35 (s, -OC***H***$_3$ in PEO end-capping), 2.90–3.10 (bs, -C***H***$_2$C***H***$_2$COCF$_3$ in PMATFK block), 1.15–1.66 (br, -C***H***$_2$C***H***- in PMATFK main chain).

^{19}F NMR (δ, ppm, $CDCl_3$): -79.3 (s)

3.3 Preparation of $ONOO^-$ and Other Reactive Oxygen and Nitrogen Species (ROS/RNS)

Peroxynitrite. $ONOO^-$ was prepared according to the literature and modified.[3] Briefly, to a solution of sodium hydroxide (30 mL, 1.5 M) was added sodium nitrite (30 mL, 0.6 M) and the mixture of hydrogen peroxide (30 mL, 0.7 M) and hydrochloric acid (0.6 M). It is noted that sodium nitrite and acidified hydrogen peroxide was added dropwise via a Y-type pipe with the same pump rate. Then activated manganese dioxide (4.0 g) was added to the resulted solution slowly to remove the excess hydrogen peroxide. After 15 min later the mixture was filtrated under reduced pressure and bright yellow filtrate was split into small aliquots and stored at lower than -18 °C. The operation of all of the above was carried out at 4 ^{o}C. The concentration of the prepared peroxynitrite was determined by testing the absorption of the solution at 302 nm. The extinction coefficient of $ONOO^-$ solution in 0.1 M NaOH is 1670 M^{-1} cm^{-1} at 302 nm. $C_{ONOO^-} = Abs_{302nm}/1.67$ (mM).

Hydrogen Peroxide. H_2O_2 (30 μM) was added to the polymer assemblies for selective responsiveness analysis.

Singlet Oxygen. $^1O_2$ was generated by (3-(1,4-dihydro-1,4-epidioxy-1-naphthyl)propi onic acid. It (30 μM) was added to the polymer assemblies with stirring at 25 ^{o}C.

Superoxide Anion. $O_2^{\bullet-}$ was generated by xanthine and xanthine oxidase. Xanthine oxidase was added firstly. After xanthine oxidase was dissolved, xanthine (30 μM) was injected to the polymer solution with stirring at 25 ^{o}C.

tert-Butyl Hydroperoxide. tBuOO$^\bullet$ (70%) solution in H_2O was diluted with PBS to gain a 30 μM stock solution, which added to the polymer solution with stirring at 25 ^{o}C.

Hydroxy Radical. $^\bullet$OH was generated by Fenton reaction between Fe^{2+} and H_2O_2. Fresh $FeCl_2$ and H_2O_2 stock solution were prepared for diluting into 30 μM.[4]

Hyperchlorite. 5% NaOCl solution was purchased from Sigma. It was diluted with PBS to gain a 30 μM stock solution. The pH was adjusted to 7.4 for adding to the polymer assemblies.

Nitric Oxide. 1-Hydroxy-2-oxo-3-(N-methyl-3-aminopropyl)-3-methyl-1-triazene stock solution (30 μM) was prepared in 0.1 M NaOH. An appropriate amount of the stock solution was added to generate NO. The final mixtures were confirmed to have no notably pH change from 7.4.[5]

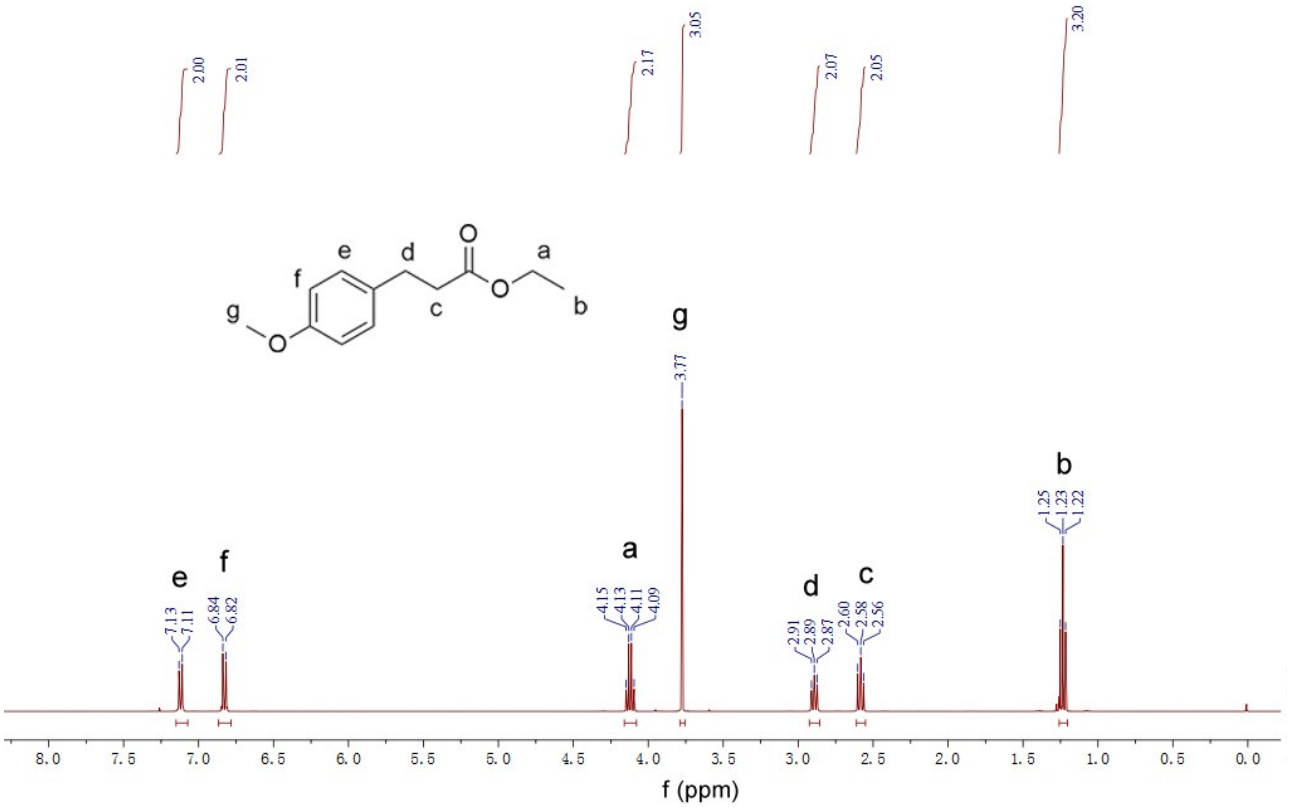

Fig. S1 ^{1}H NMR spectra for 3-(4-methoxyphenyl) propanoate in $CDCl_3$

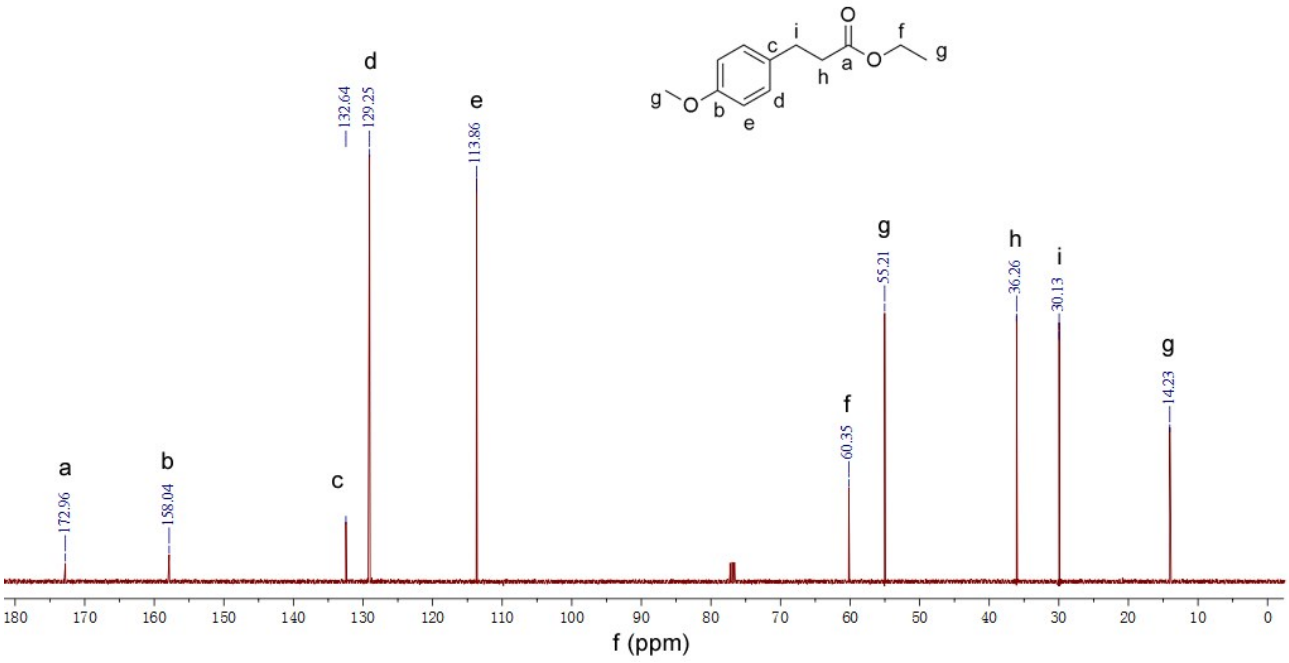

Fig. S2 ^{13}C NMR spectra for 3-(4-methoxyphenyl) propanoate in $CDCl_3$

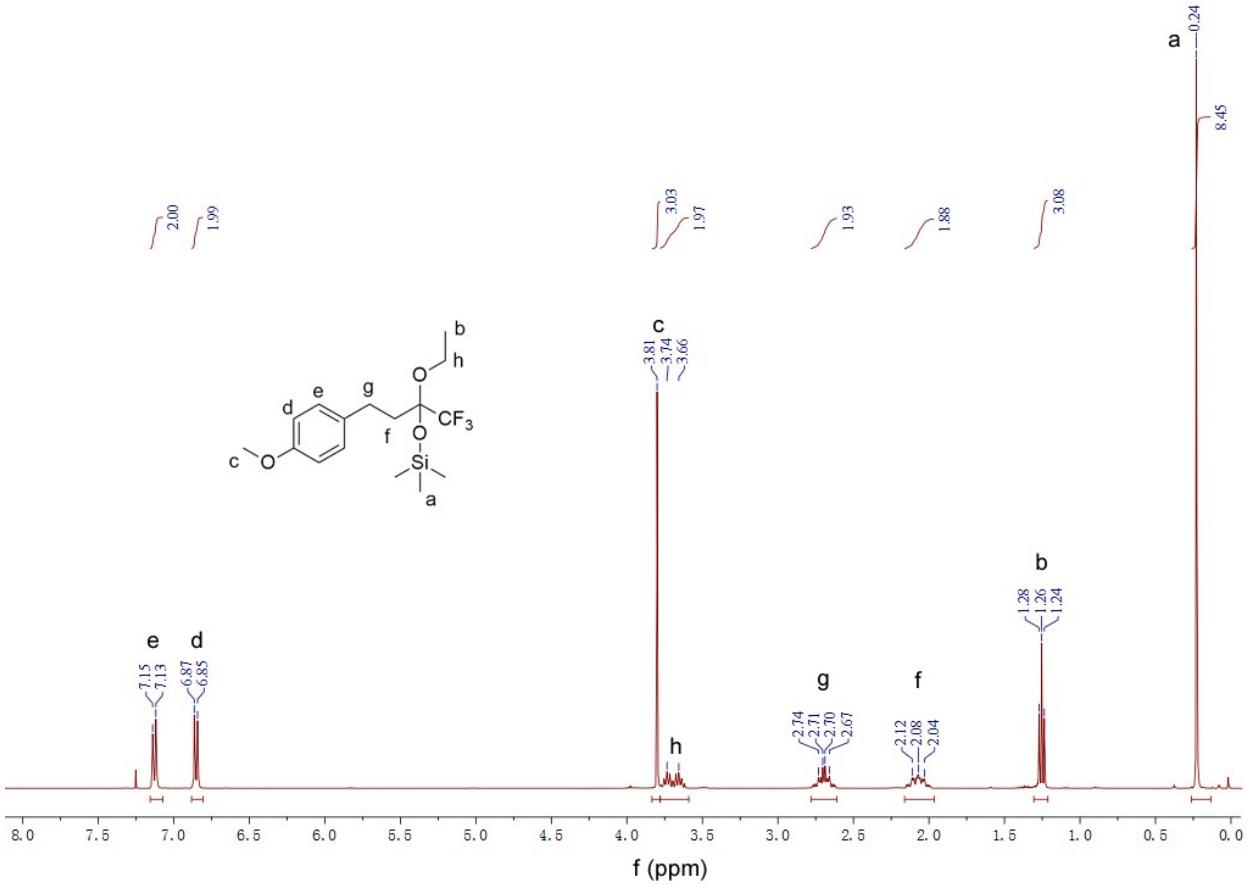

Fig. S3 ^{1}H NMR spectra for (2-ethoxytrifluoro-(4-methoxyphenyl)butan-2-yl) trimethylsilane in $CDCl_3$

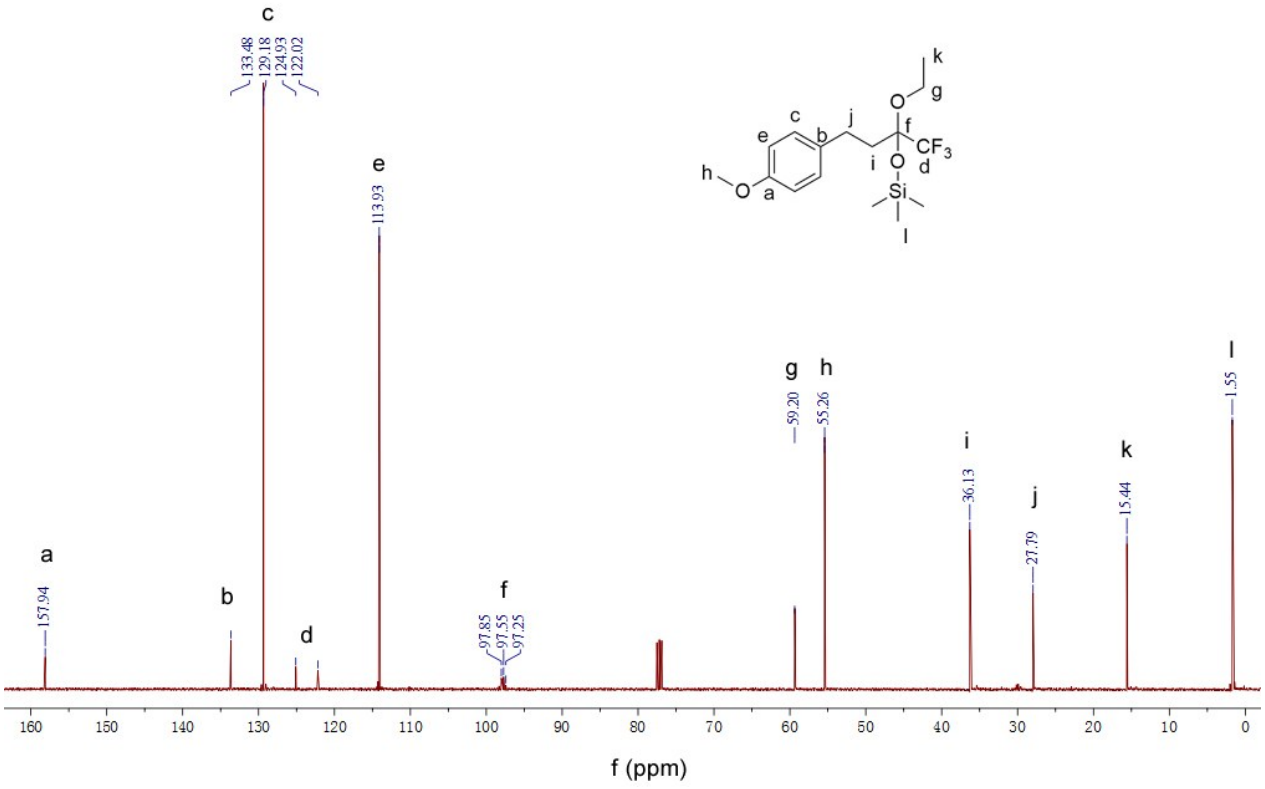

Fig.S4 ^{13}C NMR spectra for (2-ethoxytrifluoro-(4-methoxyphenyl)butan-2-yl) trimethylsilane in $CDCl_3$

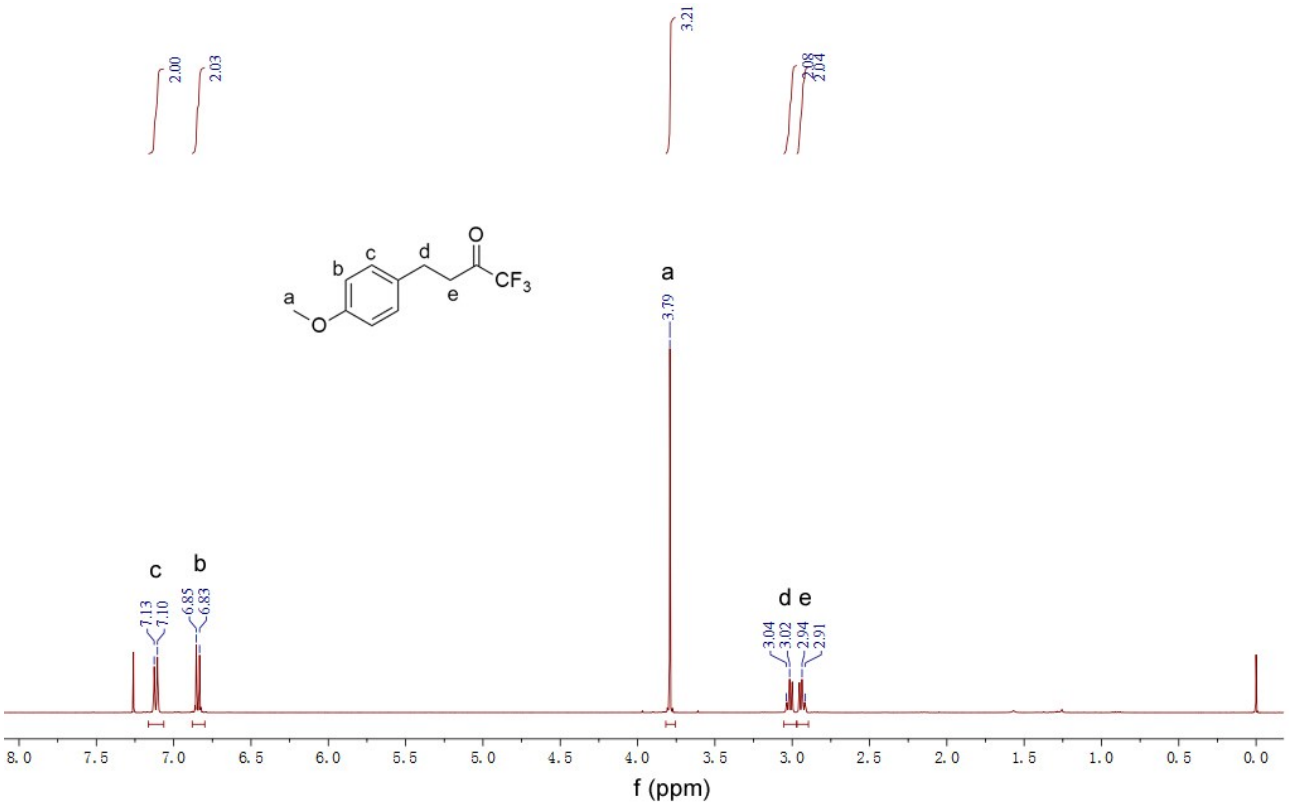

Fig. S5 ^{1}H NMR spectra for trifluoro-4-(4-methoxyphenyl) butan-2-one in $CDCl_3$

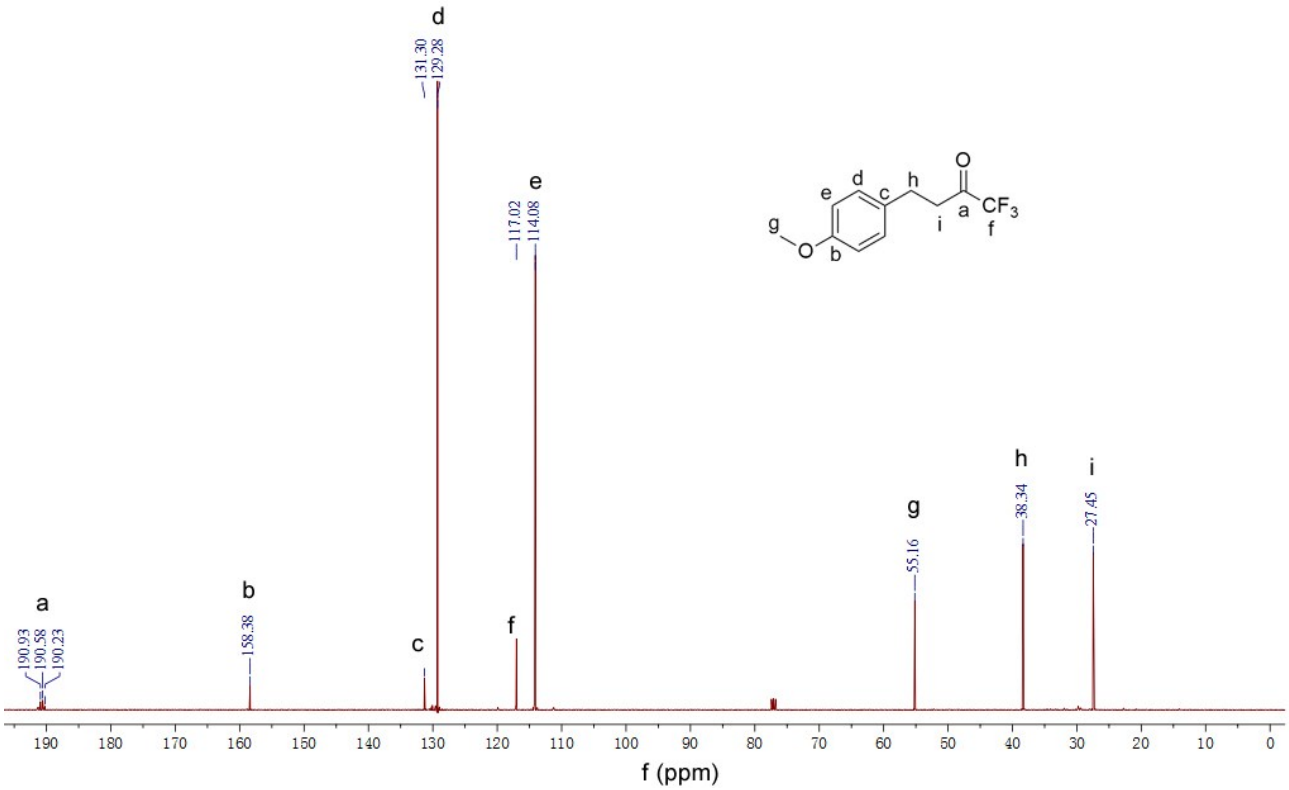

Fig. S6 ^{13}C NMR spectra for trifluoro-4-(4-methoxyphenyl) butan-2-one in $CDCl_3$

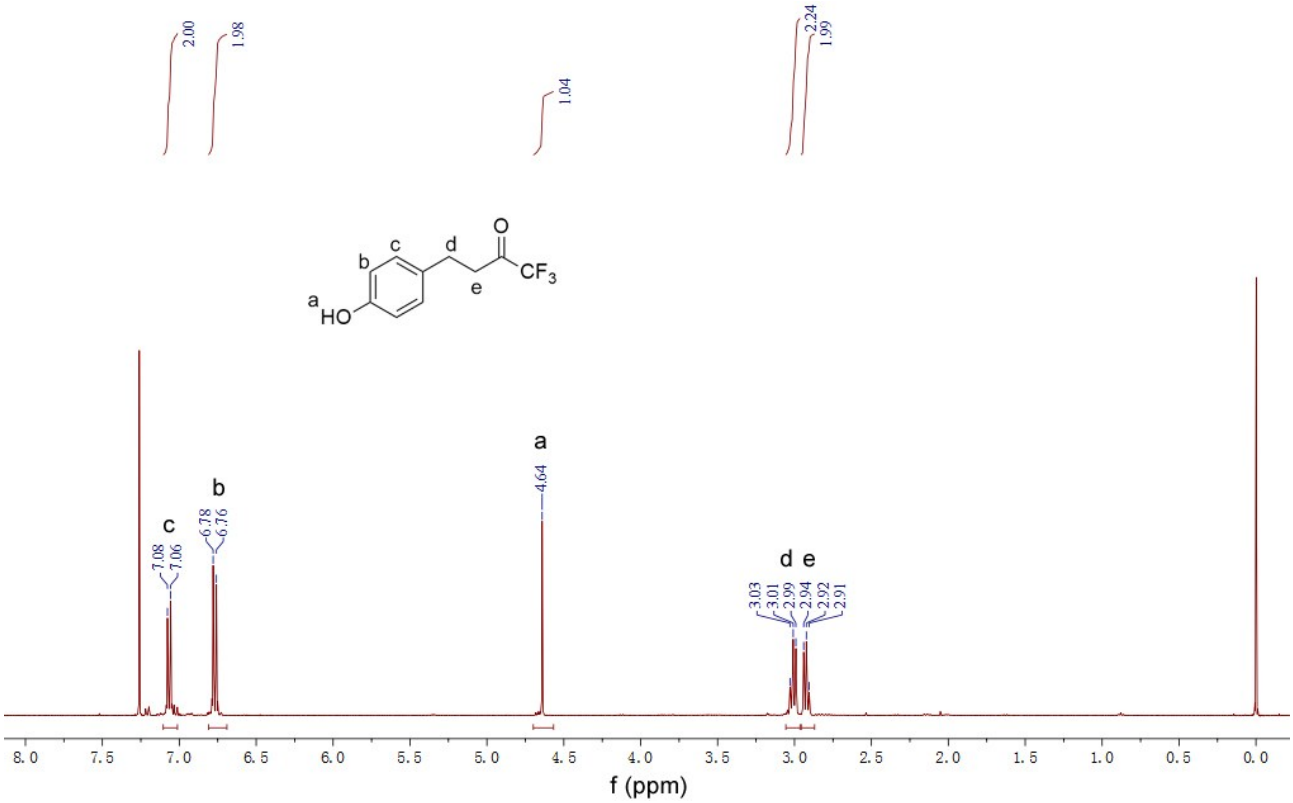

Fig. S7 ^{1}H NMR spectra of trifluoro-4-(4-hydroxyphenyl) butan-2-one in $CDCl_3$

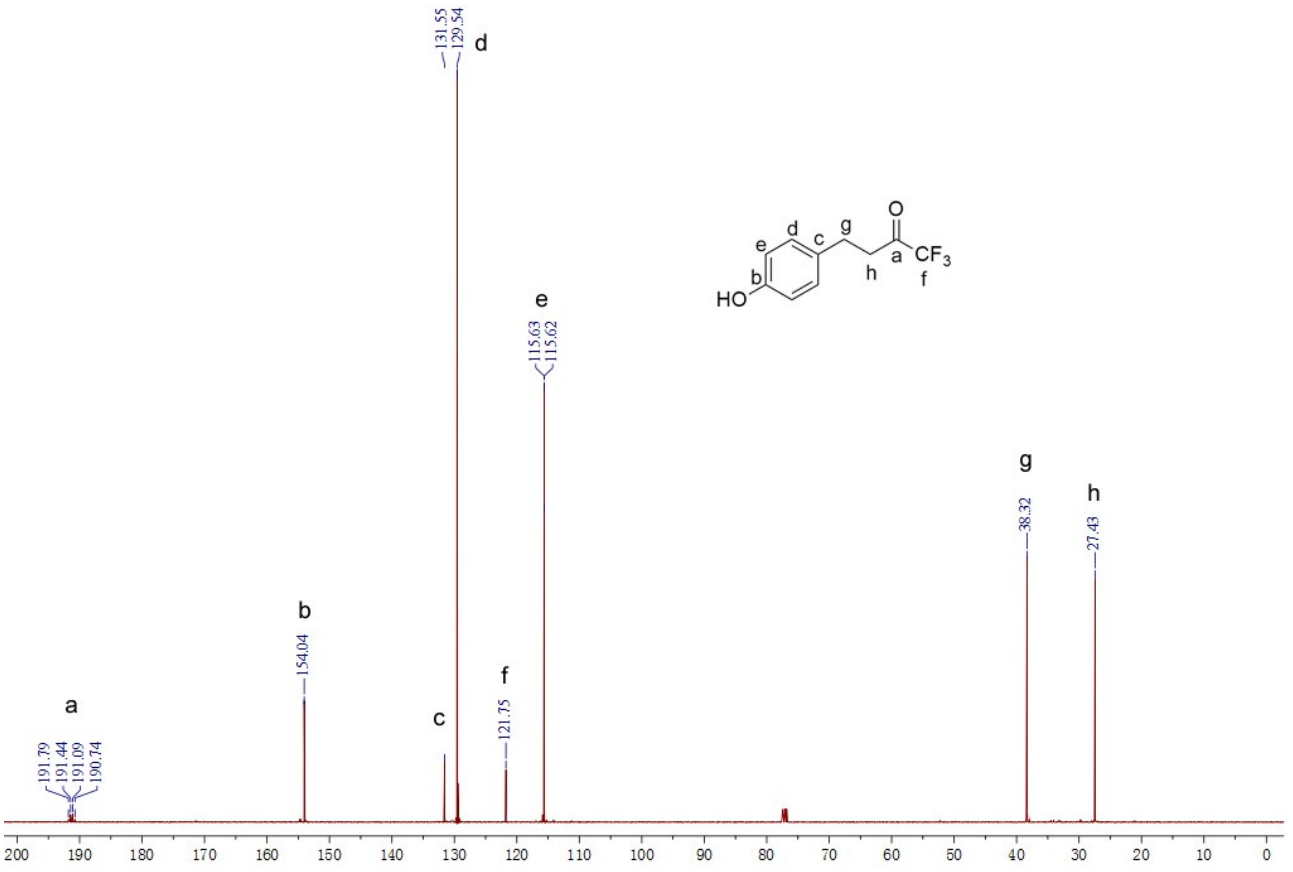

Fig. S8 ^{13}C NMR spectra of trifluoro-4-(4-hydroxyphenyl) butan-2-one in $CDCl_3$

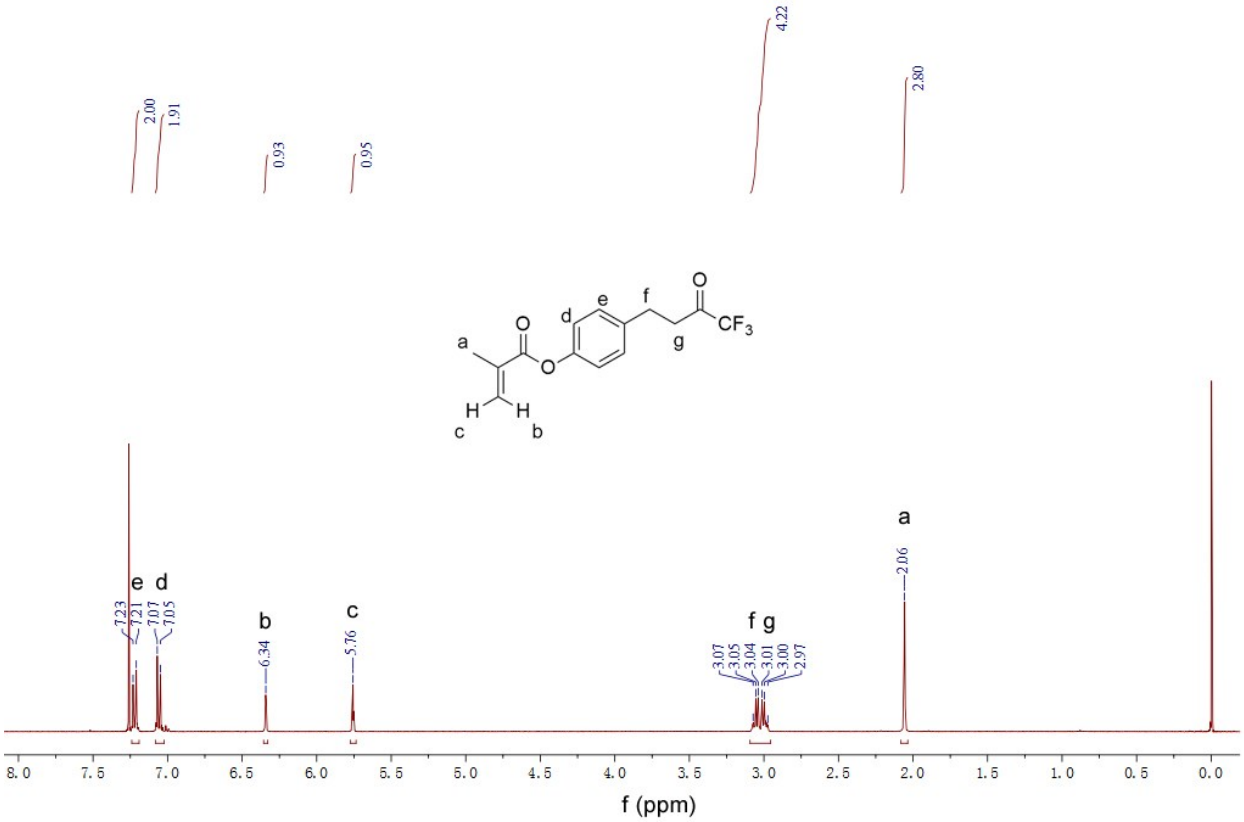

Fig. S9 ^{1}H NMR spectra of functional monomer 4-(trifluoro-3-oxobutyl) phenyl methacrylate (MATFK) in $CDCl_3$

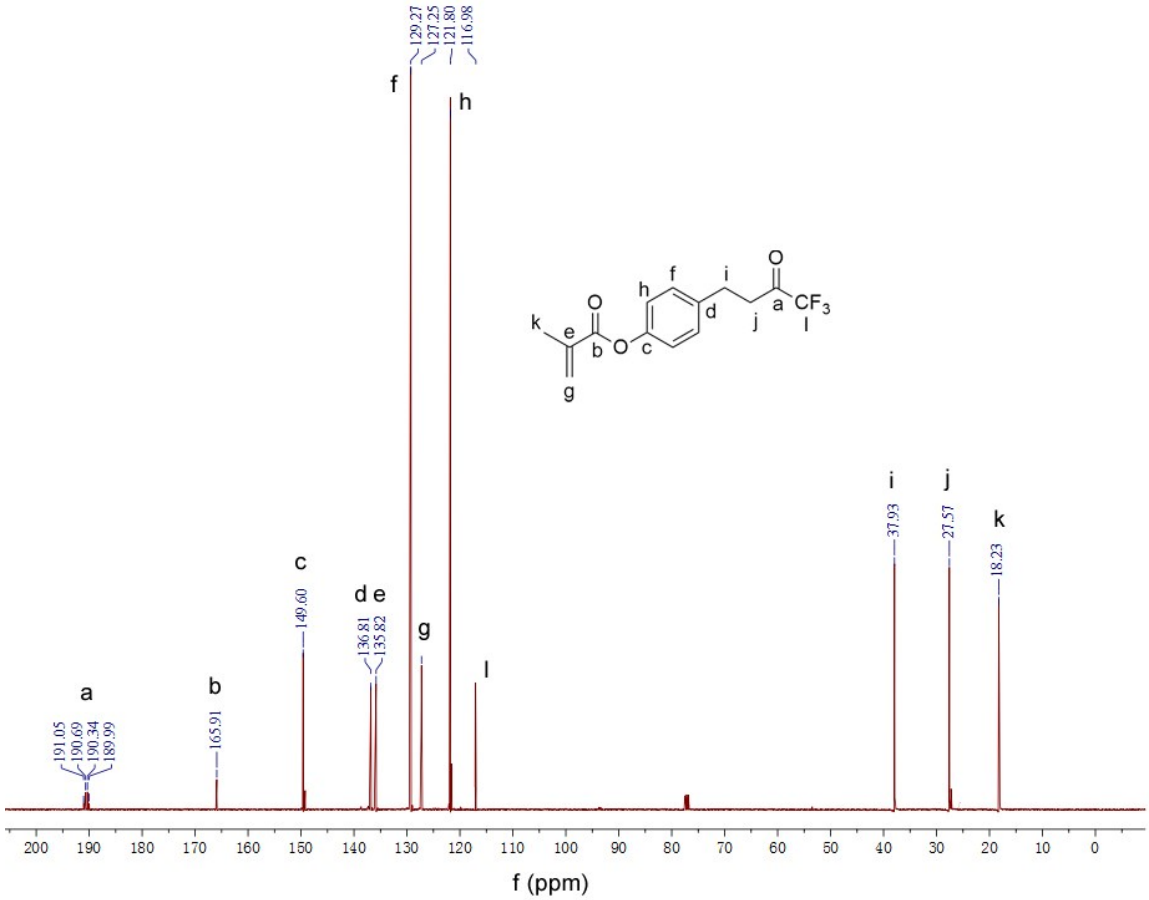

Fig. S10 ^{13}C NMR spectra of functional monomer 4-(trifluoro-3-oxobutyl) phenyl methacrylate (MATFK) in $CDCl_3$

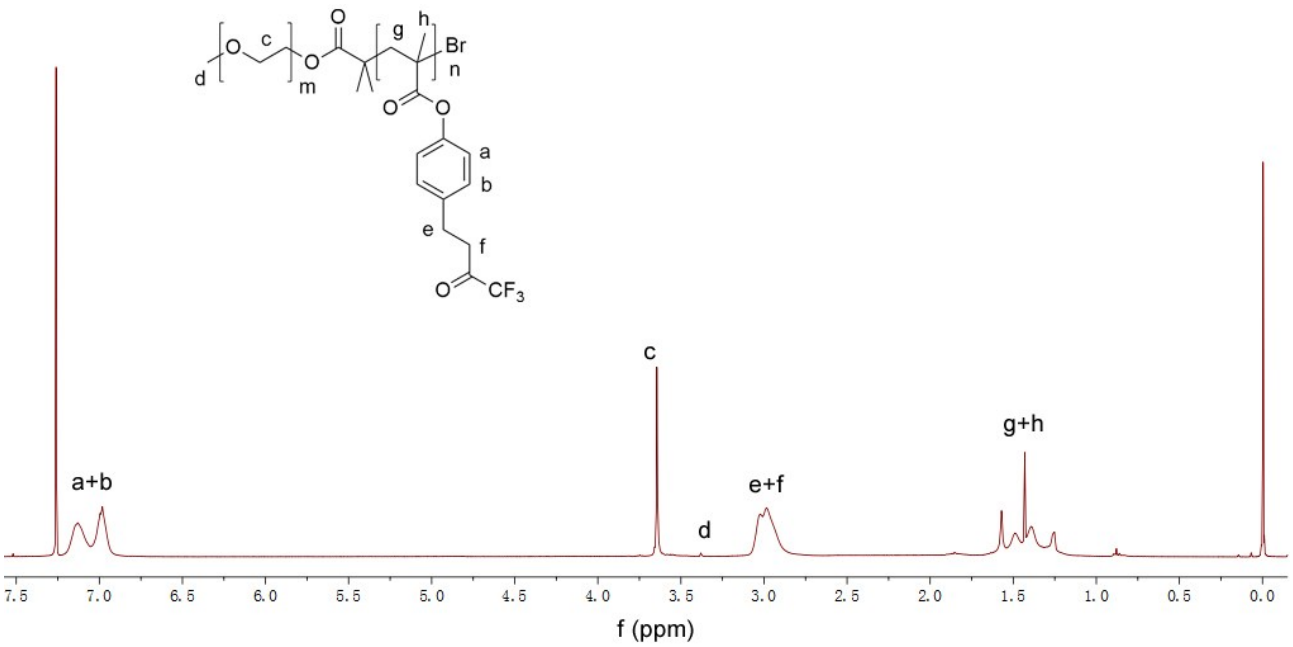

Fig. S11 ^{1}H NMR spectra for PEO-*b*-PMATFK block copolymer in $CDCl_3$

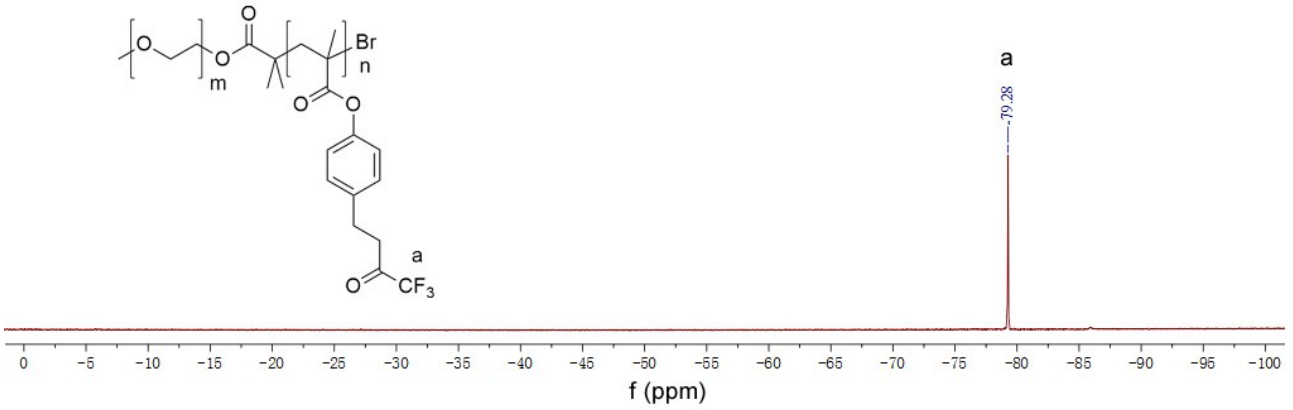

Fig. S12 ^{19}F NMR spectra for PEO-*b*-PMATFK copolymer in $CDCl_3$

Table S1. Summary of the Structural Parameters of $ONOO^-$-Responsive PEO-*b*-PMATFK and PEO-*b*-P(MATFK-*co*-TMF) Block Copolymers

Samples	**Time/h**	M_n[a]**/kDa**	M_w/M_n	D_h[b]**/nm**	**Morphology**[c]
PEO_{45}-*b*-$PMATFK_{16}$	6	7.3	1.27	17	irregular
PEO_{45}-*b*-$PMATFK_{27}$	10	10.1	1.45	42.6	sphere
PEO_{45}-*b*-$PMATFK_{49}$	24	16.4	1.46	>150	cylinder
PEO_{45}-*b*-P($MATFK_{0.92}$-*co*-$TMR_{0.08}$)$_{31}$	12	11.8	1.41	41.3	sphere

[a] Determined by GPC using DMF as the eluent at a flow rate of 1.0 mL min^{-1} at 30 ^{o}C; [b] Determined by DLS at room temperature; [c] The aggregate geometry determined by TEM images

3. Site-Specific Cleavage of MATFK Monomer by $ONOO^-$.

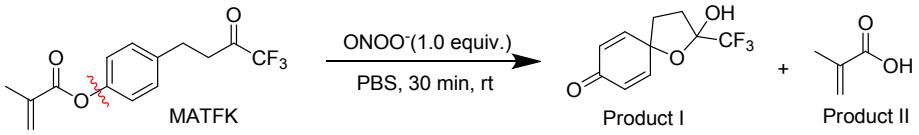

…… (1)

To further elucidate whether MATFK functional monomer can react with $ONOO^-$ stimulus and what the reaction mechanism is, we employed ESI-MS and NMR to ensure the chemical structures of the products. From the results of mass spectra (*Figure S13*), the molecule weight of MATFK functional monomer was found in 287.0899 [$M+H^+$]. When MATFK was reacted with equivalent molar $ONOO^-$ for 30 min, we can separated and purified two kinds of products. The molecular weight of product I was 235.0528 [$M+H^+$], which is corresponding to 2-hydroxyl-2-trifluoromethyl spiro-dienone.[6] The other product had a smaller molecular weight of 87.0498 [$M+H^+$]. Combining with its ^1H NMR spectrum (*Figure S14*), we could confirm that the product II is methacrylic acid (MAA). These results illustrate that $ONOO^-$ is able to facilitate an intramolecular epoxidation to attack the adjacent aromatic ring, as a result, specifically cleave the MATFK monomer at the site of phenyl ester bond, further yielding two products, 2-hydroxyl-2-trifluoromethyl spiro-dienone and MAA, respectively, as Eq.(1).

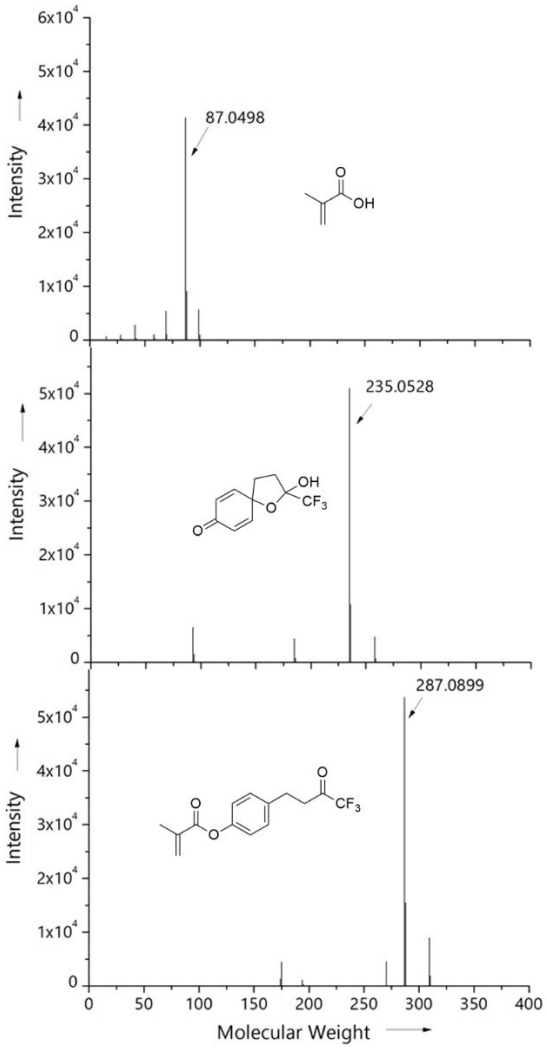

Fig. S13 ESI-MS results of MATFK monomer upon treatment with $ONOO^-$ (1.0 equiv.) for 30 min: substrate MATFK (bottom), product I (2-hydroxyl-2-trifluoromethyl spiro-dienone, middle) and product II (methacrylic acid, top)

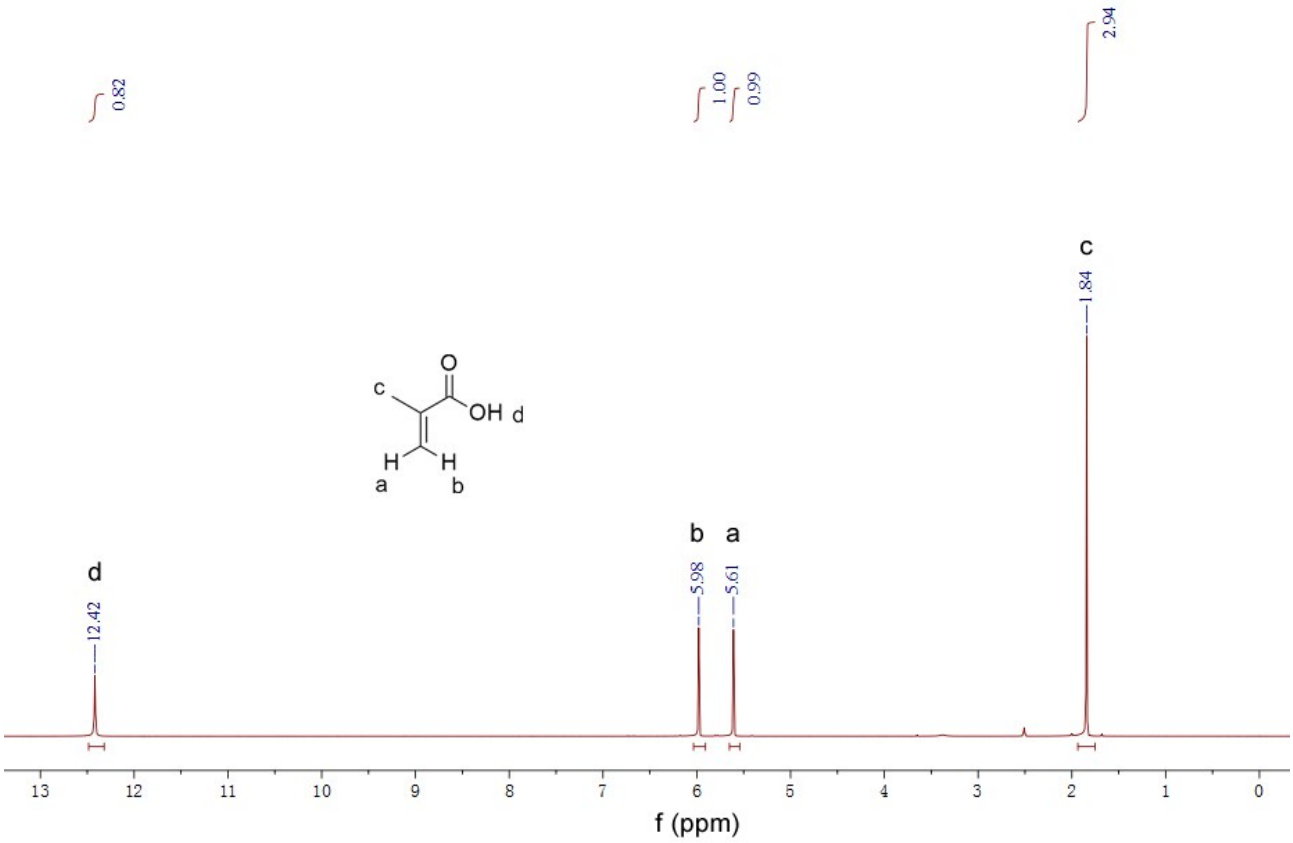

Fig. S14 ^{1}H NMR spectrum of Product II obtained from the reaction between MATFK monomer and $ONOO^-$ in d_6-DMSO solvent, which is corresponding to the chemical structure of methacrylic acid (MAA).

4. The Side Group Cleavage of PEO-*b*-PMATFK Copolymer by $ONOO^-$.

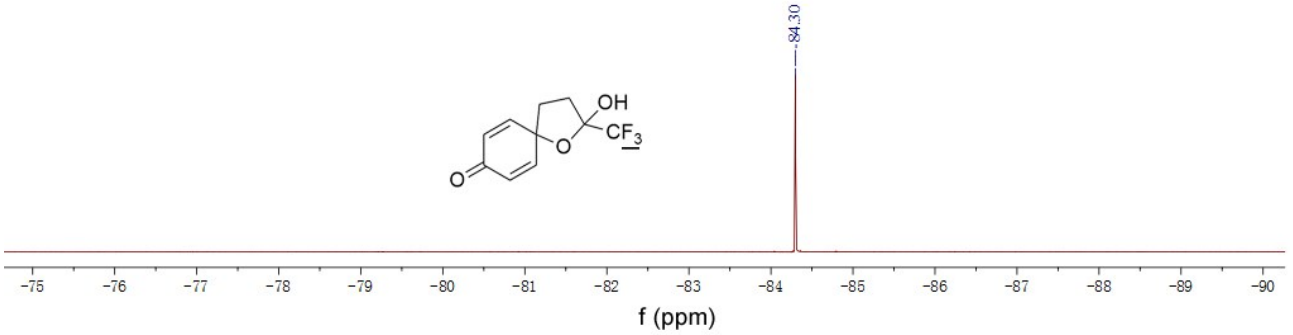

Fig. S15 ^{19}F NMR spectrum of trifluoromethyl spiro-dienone in $CDCl_3$

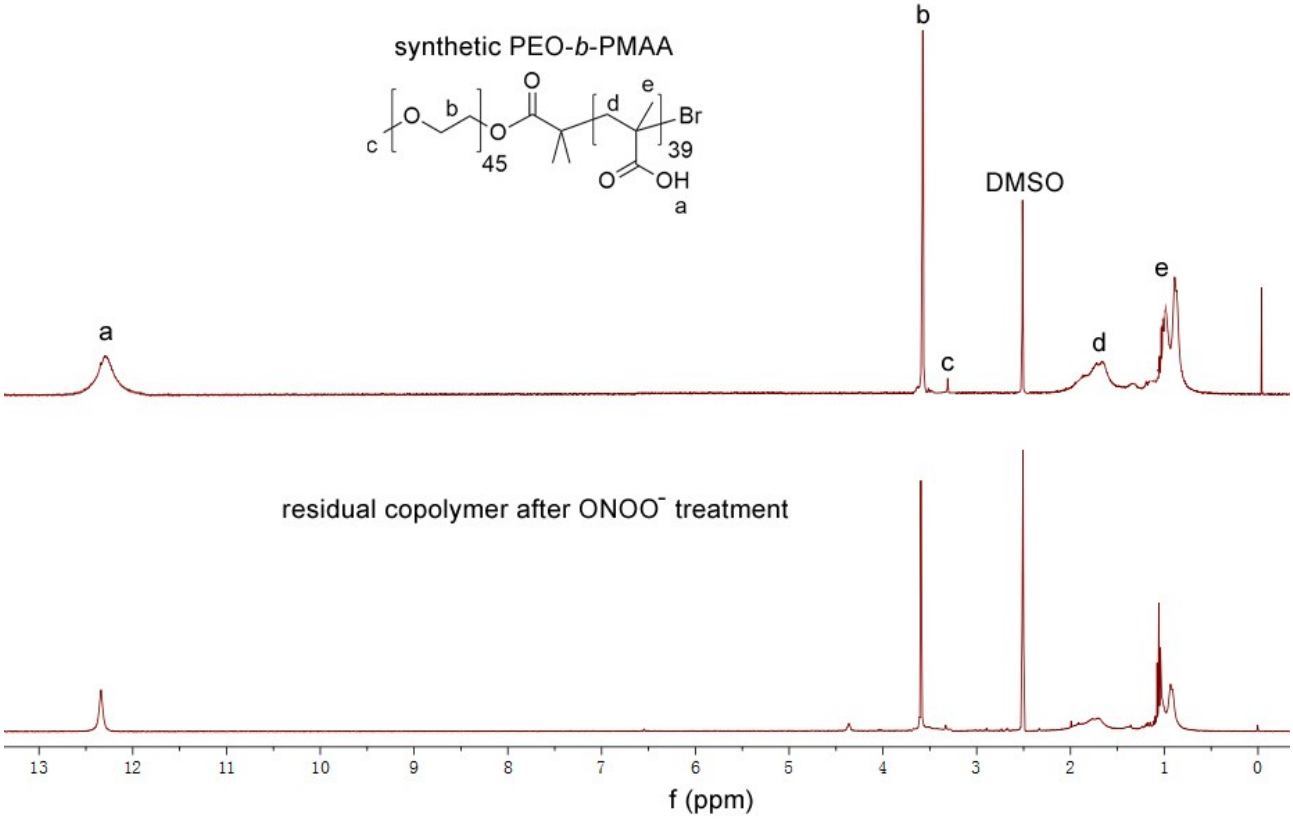

Fig. S16 ^1H NMR spectra comparison between the residual copolymer after reacted with $ONOO^-$ and the synthetic PEO-*b*-PMAA block copolymer counterpart. The similar NMR profile indicates that PEO-*b*-PMATFK reacted with $ONOO^-$ can yield water-soluble PEO-*b*-PMAA.

We envisaged that $ONOO^-$ sensitive monomer could be introduced into the block copolymer PEO-*b*-PMATFK for responsive cleavage. To elucidate this, time-resolved ^{19}F NMR experiment was carried out. In the absence of $ONOO^-$, the copolymer displayed a single fluorine signal of trifluoromethyl ketone group at δ = -79.3 ppm, corresponding to the MATFK monomer. After injecting $ONOO^-$, this peak was gradually weakened while an upfield fluorine signal at δ = -84.3 ppm elevated, which is in line with that of trifluoromethyl spiro-dienone form (*Figure S15*).[6] It indicates that our copolymer PEO-*b*-PMATFK can react with $ONOO^-$ and disconnect the MATFK side groups to form the product of trifluoromethyl spiro-dienone. Since MATFK monomer can react with $ONOO^-$ to produce MAA

and trifluoromethyl spiro-dienone, we deduced that PEO-*b*-PMATFK reacting with $ONOO^-$ can yield PEO-*b*-PMAA copolymer. To demonstrate this, we purified the resulting copolymer and analyzed its chemical structure by ^1H NMR. PEO-*b*-PMATFK is a yellow solid and has low solubility in water, however, the residual copolymer is white powder and well water-soluble. From ^1H NMR spectra, only the ethylidene proton peak (δ = 3.64 ppm) ascribed to PEO segment and polymer skeleton proton peak in upfield region (δ = 0.9–1.4 ppm) retained, but the aromatic peaks ascribed to MATFK side group totally vanished. Interestingly, a broad proton signal at downfield (δ = 12.3 ppm) was observed, which is consistent with the active proton peak of PMAA. We also synthesized PEO-*b*-PMAA block copolymer counterpart by ATRP method. As compared with this counterpart, the residual copolymer possess almost the same NMR profile (*Figure S16*). These findings all indicate that PEO-*b*-PMATFK can react with $ONOO^-$, as a result, leading to the formation of PEO-*b*-PMAA copolymer as Eq.(2).

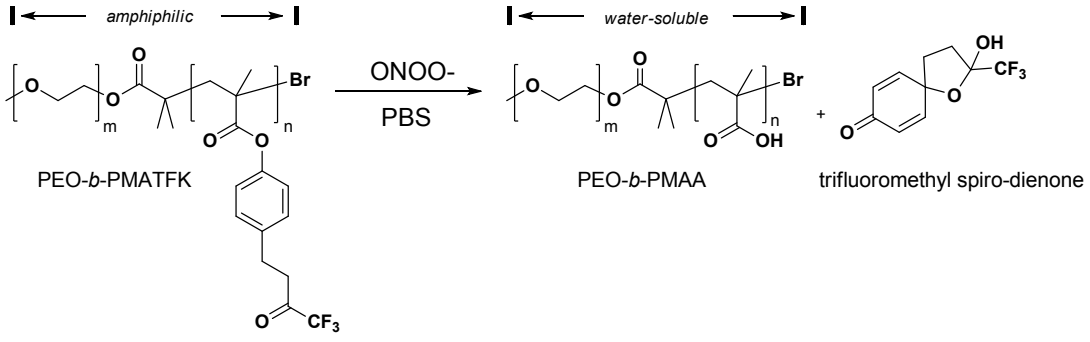

…… (2)

5. Self-Assembly Behavior and $ONOO^-$ Responsiveness of PEO-*b*-PMATFK.

5.1 The Critical Aggregate Concentration (CAC) of PEO-b-PMATFK Block Copolymer

A stock solution of 5.0 mg mL^{-1} PEO-*b*-PMATFK in THF (1 mL) was added into 20 mL of deionized water under sonication, followed by dialysis against deionized water. After 48 h dialysis for removal of the organic phase, the volume of the solution was increased to ~25 mL to obtain an aggregate solution with a concentration of 0.2 mg mL^{-1} for further experiments. The CAC of PEO-*b*-PMATFK block copolymer was measured by the fluorescent probe method.[7] 10 μL of 1×10^{-3} mg mL^{-1} pyrene solution in acetone was added to PEO-*b*-PMATFK aqueous solutions with different concentrations and the solutions were sonicated for 10 min before fluorescence emission measurement. The results showed that the CAC of PEO-*b*-PMATFK was determined to be 1.2×10^{-4} mg mL^{-1} (*Figure S17*). Thus all the subsequent experiments were carried out above this CAC at the copolymer concentration of 1.8×10^{-4} mg mL^{-1} (containing 300 nM of MATFK labeled groups).

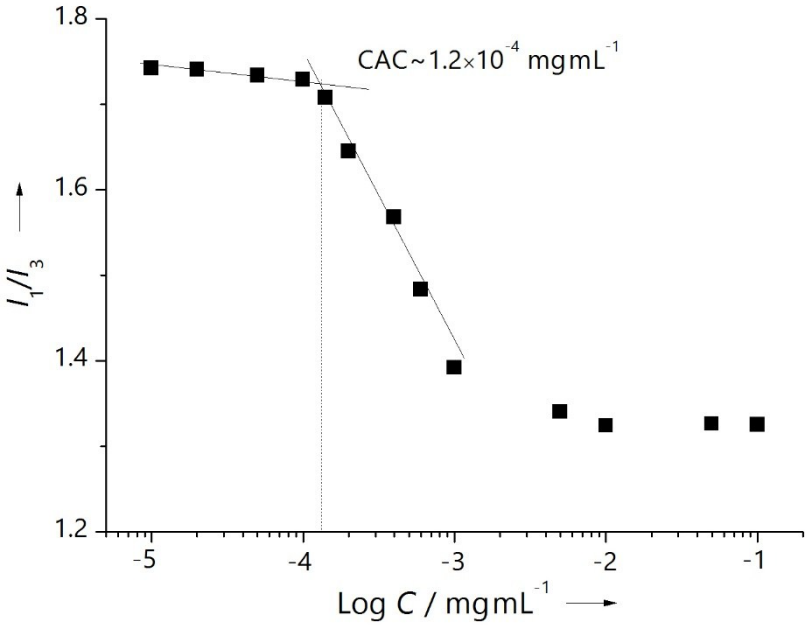

Fig. S17 Determination of CAC for the PEO-*b*-PMATFK block copolymer by using fluorescent probe method, the CAC is ca. 1.2×10^{-4} mg mL^{-1} (The CAC was chosen as the concentration when pyrene exhibited an apparent decrease in the I_1/I_3 ratio with an increasing concentration of the block copolymer, indicating that the aggregation of the copolymer)

5.2 $ONOO^-$ Concentration-Dependent Disassembly Rates of PEO-b-PMATFK Micelles

The PEO-*b*-PMATFK copolymer micelles can disassemble upon $ONOO^-$ stimulus. We doubted that this disassembly behavior is relied on $ONOO^-$ concentration. To elucidate this, turbidity experiments were carried out via UV-Vis spectroscopy (*Figure S18*). It is clear when adding 1.0 equiv. $ONOO^-$ into the micellar solution, the solution transmittance increased rapidly from 23% to 94% within only 60 min, which results from the formation of water-soluble PEO-*b*-PMAA unimers. With decreasing the $ONOO^-$ concentrations from 1.0 equiv. to 0.4 equiv., the increase of solution transmittance gradually slowed down from 60 min to 180 min. This result indicates that the micellar dissociation is $ONOO^-$ concentration-dependent.

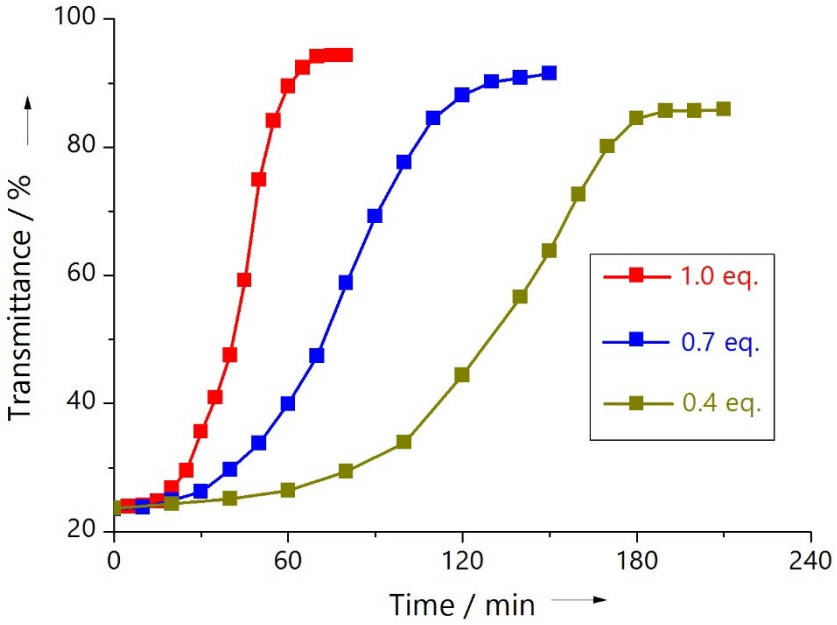

Fig. S18 Micellar solution turbidity variation plotted against reaction time at different $ONOO^-$ concentration conditions: 300 nM (1.0 equiv., ■), 210 nM (0.7 equiv., ■) and 120 nM (0.4 equiv., ■). The polymer concentration is 1.8×10^{-4} mg mL^{-1}, containing 300 nM of MATFK labeled groups.

6. Biological Selective Responsiveness of PEO-*b*-PMATFK Micelles.

We have demonstrated that our PEO-*b*-PMATFK micelles possesses $ONOO^-$-triggered disassembly ability. Because we expected that these smart micelles could be applied in physiological environment, thus they should possess highly biological specificity and selectivity to intracellular $ONOO^-$ species. However, besides $ONOO^-$ signaling molecule, there are a series of redox-active reactive oxygen and nitrogen species (ROS/RNS) coexisting in cells such as hydrogen peroxide (H_2O_2), singlet oxygen ($^1O_2$), superoxide anion ($O_2^{\bullet-}$), alkyl peroxide ($ROO^\bullet$), hydroxyl radical ($^\bullet OH$), hypochlorous acid (OCl^-), and nitric oxide (NO). To detect whether they have similar responsiveness, we used UV-Vis spectroscopy to monitor their reactivity to the PEO-*b*-PMATFK copolymer micelles. From the above results, it is known that if an irritant can cleave the labeled groups, the typical absorption band of MATFK at 278 nm will be depressed but the 2-hydroxyl-2-trifluoromethyl spiro-dienone absorption band at 246 nm will increase. Based on this, we could calculate the change of the absorption intensity as Eq. (3) in order to evaluate the reactive efficiency.

$$R\% = \frac{\Delta A_{278}}{A_{278}} \times 100\% \quad \text{.....(3)}$$

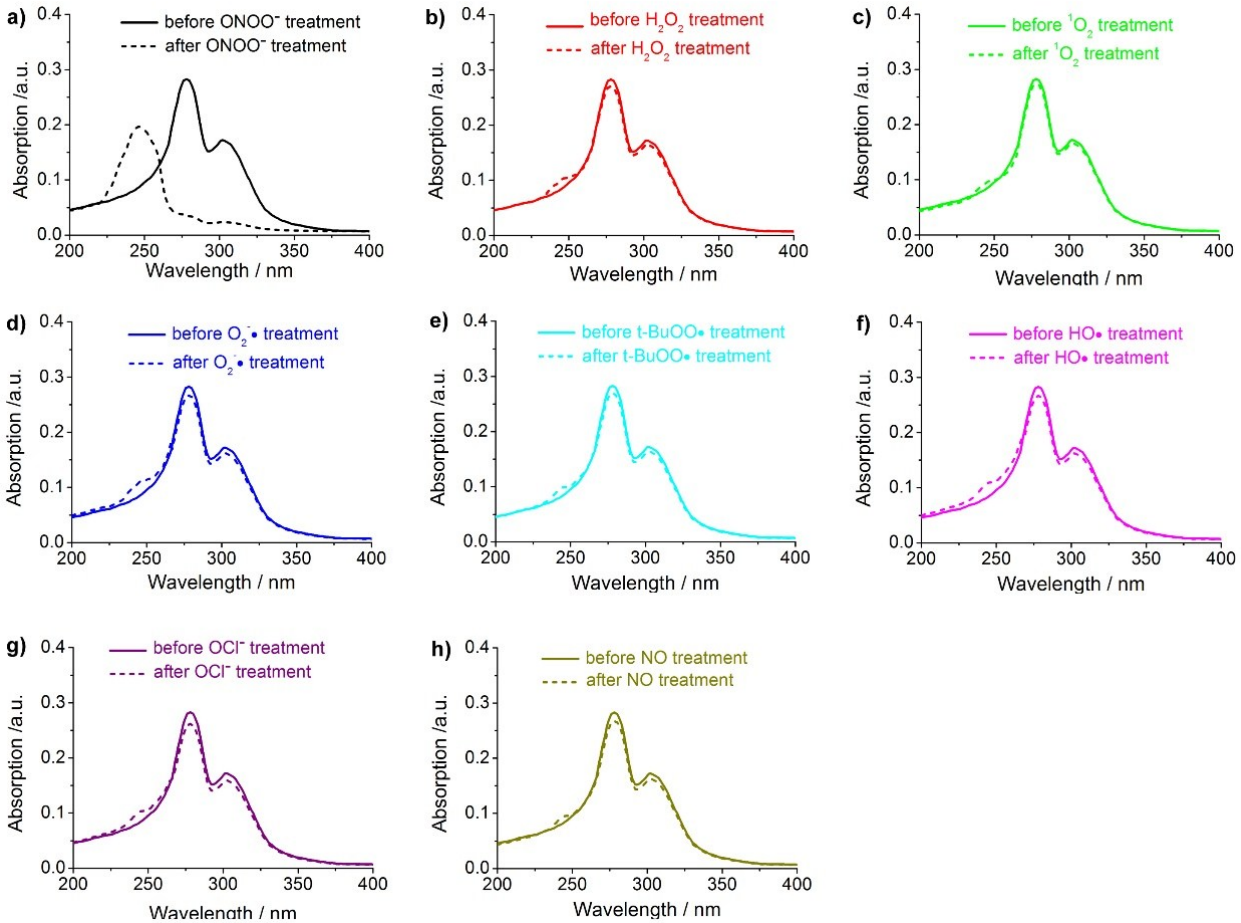

Fig. S19 UV-Vis spectra changes of PEO-*b*-PMATFK micellar solution before and after different stimuli: a) $ONOO^-$ (300 nM, 1.0 equiv.; incubation time kept 1 h and the reactivity as 100% reference), b) H_2O_2 (reactivity is 4.4%), c) $^1O_2$ (reactivity is 3.6%), d) $O_2^{\bullet-}$ (reactivity is 5.8%), e) *t*-$BuOO^\bullet$ (reactivity is 4.7%), f) $^\bullet OH$ (reactivity is 5.2%), g) OCl^- (reactivity is 7.1%), h) NO (reactivity is 4.5%). All of the ROS/RNS levels are kept at 30 μM, 100 equiv. and the incubation time prolonged

to 12 h.

As shown in *Figure S19a*, we found that $ONOO^-$ causes the decomposition of PEO-*b*-PMATFK. When we regarded $ONOO^-$ irritant as 100% activity, in a similar way, adding other biological stimulants into our polymer vesicle system (concentration is 30 μM, 100 equiv.) for half a day led to negligible UV-Vis changes (*Figure S19b*, H_2O_2; *Figure S19c*, $^1O_2$; *Figure S19d,* $O_2^{\bullet-}$; *Figure S19e*, *t*-$BuOO^{\bullet}$; *Figure S19f,* $^{\bullet}OH$; *Figure S19g*, OCl^-; *Figure S19h*, NO). These findings confirmed that other ROS and RNS have no ability to induce the polymer micellar disassembly and demonstrate that our polymer assemblies are of high-specific $ONOO^-$-responsiveness.

7. The Possible Mechanism of $ONOO^-$-Dependent Fluorescent Sensing.

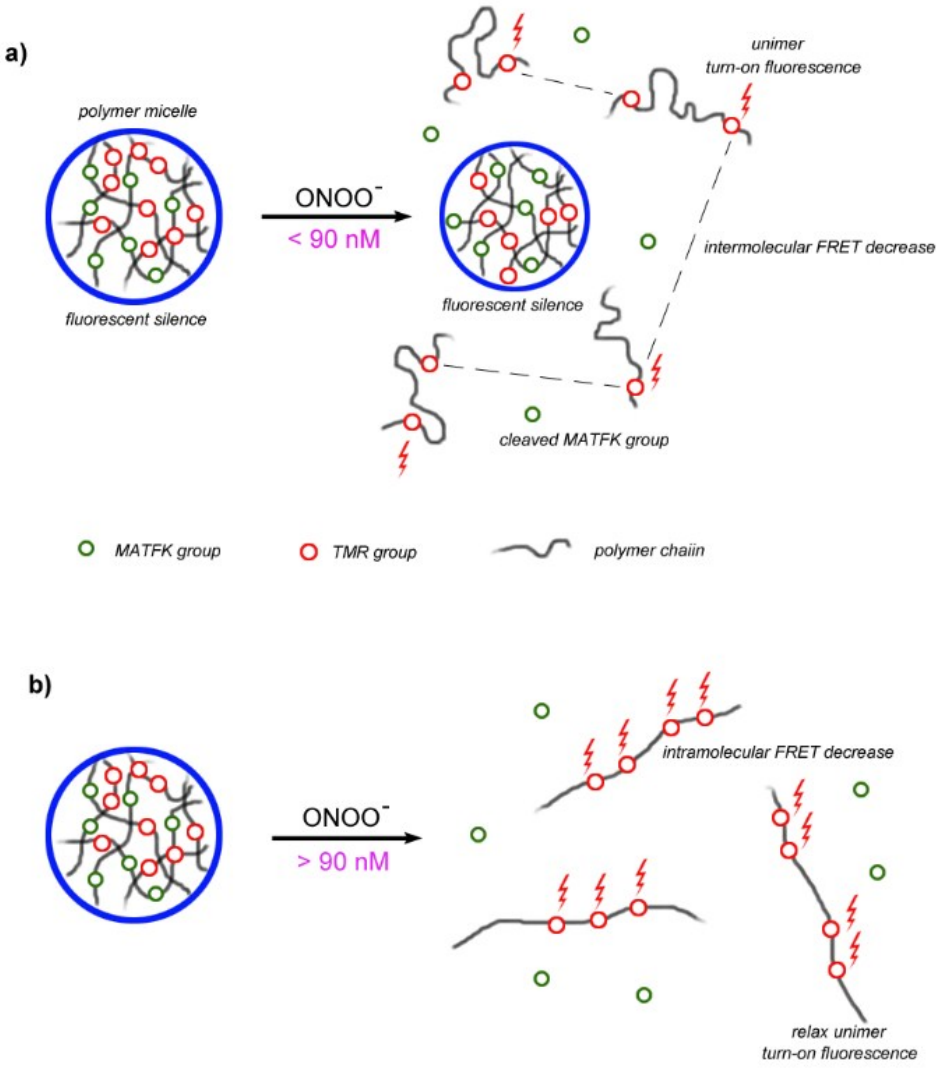

Fig. S20 The possible mechanisms of the polymer micellar nanoparticle showing $ONOO^-$-dependent fluorescent sensing a) below and b) upper its LCDT.

From the micellar dissociation experiment by DLS, it was found that the polymer micelles can be disassembly upon $ONOO^-$ stimulus, and the lowest critical dissociation threshold (LCDT) is determined to be 90 nM (0.3 equiv. with respect to the MATFK group in polymer chain). This means that if the $ONOO^-$ concentration is over 90 nM, an apparent state is that almost all of the micelles are dissociation; on the contrary, if the $ONOO^-$ level is lower than 90 nM, an apparent phenomenon is that the micelles remain their spherical structure but give a small size decrease. In view of these, we deduced that the ONOO-sensitive fluorescent mechanism of our polymer micelles is as follows. Below the LCDT (<90 nM), the $ONOO^-$ detection mechanism arises from a fluorescent turn-on of the small amount dissolved unimers escaped from the micellar core. In the absence of $ONOO^-$, the micelles are small and tight (~40 nm), which leads to the adjacency of TMR fluorophores in different polymer chains. According to Förster resonance energy transfer theory, it is known that the quite small distance of two fluorophores can cause fluorescent quenching. Thus, the micelles show fluorescent silence. However, when adding a little $ONOO^-$ (0~90 nM), although the micelles are not

completely dissociation, there are also a small amount of polymer chains that respond to $ONOO^-$ and disassemble from the internal core. These unimers in solution can turn on the TMR fluorescence because the distance of TMR moieties increased and exceeded the intermolecular Förster resonance energy transfer distance (as shown in new ***Figure S20a***). Moreover, with the increase of $ONOO^-$ level, the number of unimers has a gradual increase, which results in the enhancement of TMR fluorescent intensity. Upper the LCDT (>90 nM), the $ONOO^-$ detection mechanism is derived from the decrease of intramolecular Förster resonance energy transfer. That is to say, when $ONOO^-$ level is over 90 nM, the micelles can be nearly complete disrupted into unimers. The contribution of fluorescent enhancement from the reduction of intermolecular Förster resonance energy transfer (different unimers) seems to be the same. However, the higher concentration $ONOO^-$ is, the higher cleavage efficiency of MATFK group can be obtained. Thus, the higher $ONOO^-$ level can give rise to more soluble unimer with relax chain conformation, which further causes the decrease of intramolecular Förster resonance energy transfer; as a result, the polymer fluorescence show a further increase with $ONOO^-$ concentration increase (as shown in new ***Figure S20b***). It is clear that the fluorescent detection mechanisms are different before and after the micellar dissociation, but they together lead to a result of near-linear fluorescent increase.

8. $ONOO^-$ Detection Limit of PEO-*b*-P(MATFK-*co*-TMR) Micellar Nanoparticles.

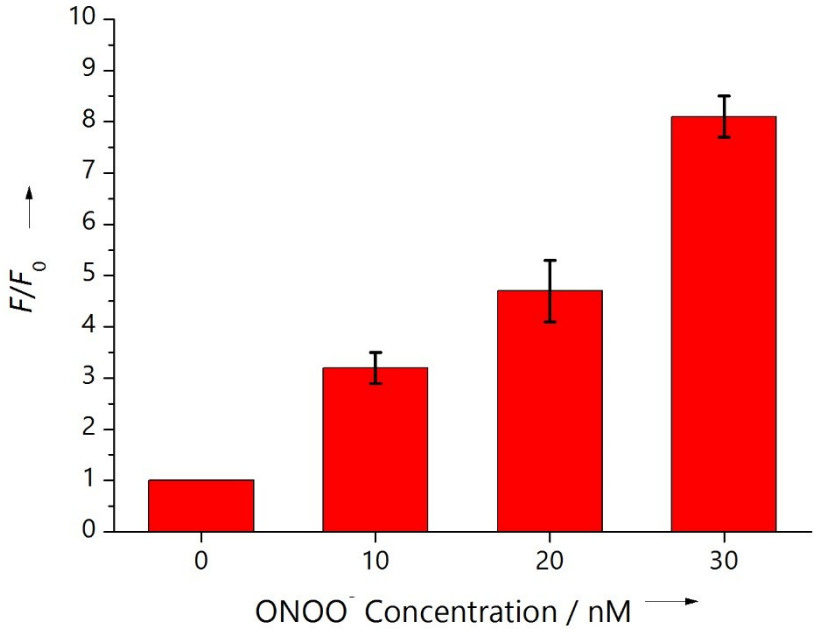

Fig. S21 Detection limit of PEO-*b*-P(MATFK-*co*-TMR) micelle nanoparticle (1.8×10^{-4} mg mL^{-1}, containing 300 nM of MATFK labeled groups). The copolymer solution in PBS (pH = 7.4) was treated with various concentrations of $ONOO^-$ and the fluorescent intensity at emission maxima (λ_{em} = 575 nm) was recorded and the detection limit was determined to be the concentration of $ONOO^-$ that induced a 3-fold fluorescent increase (detection limit is ~10 nM).

9. Biological Toxicity Evaluation of PEO-*b*-P(MATFK-*co*-TMR) Micelles.

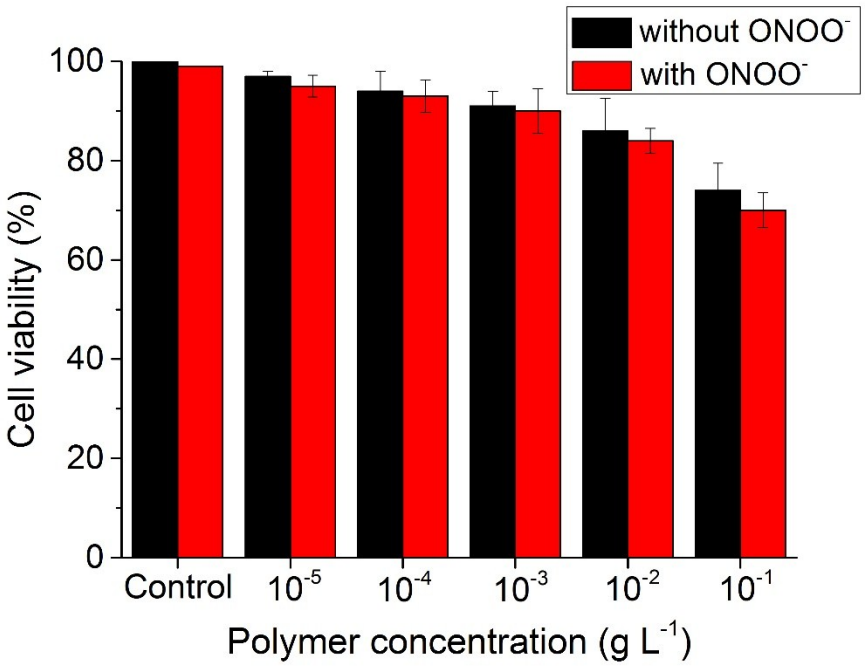

Fig. S22. MTT assays for showing the biocompatibility of PEO-*b*-P(MATFK-*co*-TMR) micelles of varied concentrations on HepG2 cell.

References

[1] J. Z. Du and Y. M. Chen, *Macromolecules* **2004**, *37*, 6322-6328.
[2] K. J. Zhou, Y. G. Wang, X. N. Huang, K. Luby-Phelps, B. D. Sumer and J. M. Gao, *Angew. Chem. Int. Ed.*, **2011**, *50*, 6109-6114.
[3] J. W. Reed, H. H. Ho and W. L. Jolly, *J. Am. Chem. Soc.* **1974**, *96*, 1248-1249.
[4] R. V. Lloyd, P. M. Hanna and R. P. Mason, *Free Radical Biol. Med.* **1997**, *22*, 885-888.
[5] I. D. Johnson, *The Molecular Probes Handbook: A Guide to Fluorescent Probes and Labeling Technologies;* 11th ed.; Life Technologies Corporation, 2010.
[6] T. Peng and D. Yang, *Org. Lett.* **2010**, *12*, 4932-4935.
[7] P. P. Infelta, M. Gratzel, J. K. Thomas, *J. Phys. Chem.* **1974**, *78*, 190-195.